Short Communication **Open Access**

Olaf Walter*, Karin Popa*, Oliver Dieste Blanco

Hydrothermal decomposition of actinide(IV) oxalates: a new aqueous route towards reactive actinide oxide nanocrystals

DOI 10.1515/chem-2016-0018
received July 1, 2016; accepted August 23, 2016.

Abstract: The hydrothermal decomposition of actinide(IV) oxalates (*An*= Th, U, Pu) at temperatures between 95 and 250 °C is shown to lead to the production of highly crystalline, reactive actinide oxide nanocrystals (NCs). This aqueous process proved to be quantitative, reproducible and fast (depending on temperature). The NCs obtained were characterised by X-ray diffraction and TEM showing their size to be smaller than 15 nm. Attempts to extend this general approach towards transition metal or lanthanide oxalates failed in the 95-250 °C temperature range. The hydrothermal decomposition of actinide oxalates is therefore a clean, flexible and powerful approach towards NCs of AnO_2 with possible scale-up potential.

Keywords: actinide oxides, hydrothermal decomposition, nanocrystals, oxalate

1 Introduction

Nanocrystals (NCs) represent fundamental building blocks in nanoscience and nanotechnology because of their size and shape dependent properties and have attracted significant interest [1-3]. Much has been published on nanomaterials with stable elements, however due to the radioactive nature of the actinides combined with safety issues and restrictions in handling, as well as reduced availability and difficulties in access, in the case of the transuranium elements, less is published on actinide nanoparticles and then practically all on actinide dioxides (AnO_2).

An excellent knowledge on the production and properties of nanometric sized AnO_2 is essential for several reasons. They can be used as precursors for the production of materials with special properties, mimic structures which are found in spent nuclear fuels or act as models to study and understand migration in a geological environment. The migration of plutonium in the geosphere proceeds faster than predicted [4,5], indicating a colloid-facilitated transport [6]. As a consequence, a reliable and reproducible method dedicated to the controlled synthesis of actinide-based NCs is highly desirable to perform dedicated studies with respect to mobility of actinides in a well-equipped laboratory.

Furthermore, easy access to nanocrystalline AnO_2 would enable detailed studies on size dependent properties of these materials. Nanometric sized crystalline particles of AnO_2 have been reported using different synthetic routes in a limited number of publications [7-19]. Questions related to size and shape effects on physical and chemical properties of actinide nano-objects are still difficult to answer. Small crystalline NCs of AnO_2 were obtained by the decomposition of different *An*-containing compounds in highly coordinating organic media [20-24], in analogy to methods developed for transition metals [25-27].

Different aqueous processes yielding NCs of (over) stoichiometric AnO_2 were also applied [28-30]. Among them, oxalate precipitation/decomposition seems to be the most suitable route towards nanograined AnO_2. However, the so-called "low-temperature oxalate decomposition process" takes place above 600 °C in the case of U^{IV} and Th^{IV} [31]. As a result, the reactivity of such nanopowders would be decreased considerably as, at these temperatures, the aggregation and growth of the nanoparticles starts to proceed.

All the inconveniences presented by the former processes (elaborate methods for organic-driven systems, high temperature use, long reaction time) could be avoided by employing an alternative approach i.e.

***Corresponding author: Olaf Walter, Karin Popa:** European Commission, Joint Research Centre, Institute for Transuranium Elements, P.O. Box 2340, D-76125 Karlsruhe, Germany, E-mail: olaf.walter@ec.europa.eu; karin.popa@ec.europa.eu
Oliver Dieste Blanco: European Commission, Joint Research Centre, Institute for Transuranium Elements, P.O. Box 2340, D-76125 Karlsruhe, Germany

the hydrothermal decomposition of hydrated actinide oxalates. The synthesis of NCs in hot compressed water under hydrothermal conditions or other solvents is well known and established [32-34]. The production of NCs in continuous flow reactors has been applied successfully [35,36]. However, for the synthesis of AnO_2 NCs under hydrothermal conditions and their characterisation nothing has been reported in the literature up to now [12]. Accordingly, in this contribution we report on the synthesis and characterisation of AnO_2 NCs formed under hydrothermal conditions in batch reactors. Attempts to extend this general approach towards transition metal or lanthanide oxalates, however, failed in the 95-250 °C temperature range.

2 Experimental Procedure

Different amounts (30-100 mg) of $An(C_2O_4)_2 \cdot nH_2O$ (synthesis procedures described elsewhere) [31,37] were heated at 95-250 °C in 20 ml Teflon autoclaves together with a small volumes (2-5 ml) of water for 5 minutes to several days. After cooling, the autoclaves were opened and the precipitate analysed. The reaction conditions for three representative tests are given in **Table 1**. In the uranium case, the work under inert atmosphere and addition of stoichiometric amounts of hydrazine were needed to maintain the U^{IV} oxidation state.

XRD analyses were performed on a Rigaku Miniflex 600 diffractometer for the obtained ThO_2 and UO_2 NCs, whereas the PuO_2 NCs were analysed on a Bruker D8 diffractometer equipped with a LinxEye position sensitive detector. Transmission electron microscope analyses (TEM) were performed on a TecnaiG2 (FEI™) 200 kV microscope equipped with a field emission gun, modified during its construction to enable the examination of radioactive samples. The samples for the TEM investigations were prepared by dropping suspended samples on a TEM grid and evaporating the solvent. The elemental analysis of the sample during the TEM study was performed using Electron Energy Loss Spectroscopy (EELS).

3 Results and Discussions

As can be seen from the XRD data shown in **Fig. 1**, nanoparticles are formed in all cases; EELS analyses clearly proved the purity of the actinide in the AnO_2 NCs.

The particle sizes for each can be calculated from the XRD data based on the full width at half maximum for six

Table 1: Typical reaction conditions for the synthesis of AnO_2 NCs obtained through the hydrothermal decomposition of actinide(IV) oxalates, $An(C_2O_4)_2 \cdot nH_2O$.

	ThO_2	UO_2	PuO_2
Oxalate hydration degree, *n*	2	6	6
Oxalate amount, mg	66.6	86.6	32.0
Water volume, ml	5	3	5
Reaction temperature, °C	250	170	95
Reaction time, h	4	3.5	120
Colour	white	black	grass green

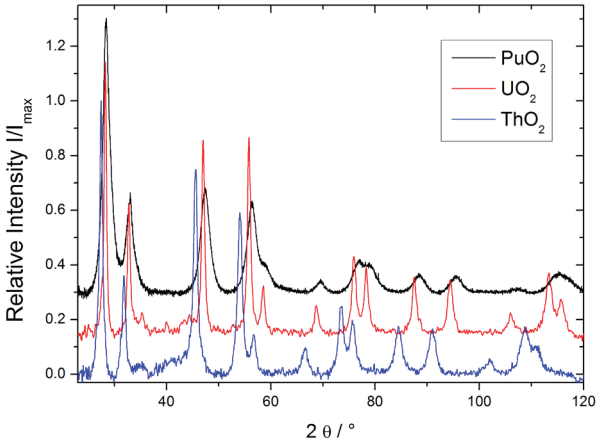

Figure 1: XRD patterns of the nanocrystalline AnO_2 obtained by hydrothermal decomposition of the corresponding oxalates; a comparison between ThO_2, UO_2, and PuO_2.

selected peaks in the 2θ range between 25 and 80° for ThO_2 and UO_2 and between 25 and 100° for PuO_2. They have been determined as 7.2(1.0) nm for ThO_2, 13.8(1.2) nm for UO_2, and 4.7(1.0) nm for the PuO_2 nanoparticles, respectively. Concerning the reactivity in the particle formation it turned out that it increases from Th to Pu, *i.e.* ThO_2 NCs can only be obtained at reaction temperatures of 250 °C, UO_2 NCs are formed at about 110 °C, whereas the PuO_2 NCs are already formed at 95 °C (but the reaction takes several days). Due to the low temperature decomposition, the size of the PuO_2 NCs is smallest, which can be derived obviously from the increased line broadening in **Fig. 1**. A more detailed size distribution analysis on the dependence on the reaction conditions has still to be concluded, as well as answering the question as to whether the decomposition has to proceed in water or whether other protic solvents or even water free systems are appropriate as well. In the case of the UO_2 NCs it is of real advantage to work under oxygen free conditions as otherwise (especially at low temperatures and long reaction times) oxidation of the U^{IV} to $UO_2(OH)_2$ might proceed. Furthermore, it is essential, in

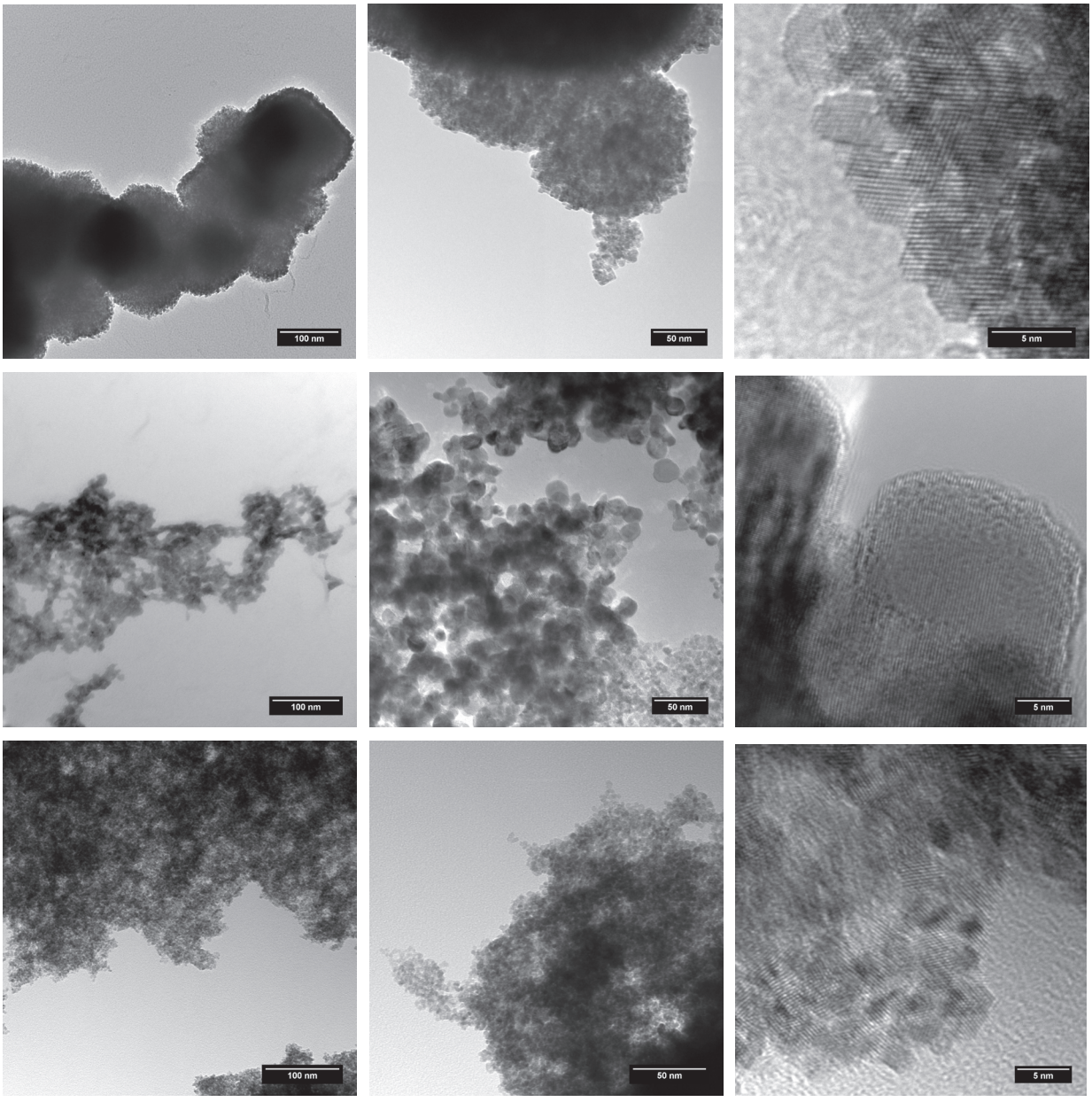

Figure 2: TEM pictures of nanocrystalline AnO_2 obtained by hydrothermal decomposition of the corresponding oxalate; a comparison between ThO_2 (top), UO_2 (middle) and PuO_2 (bottom).

order to control the size of the UO_2 NCs, to work in a non-oxidising environment.

From the TEM analyses (**Fig. 2**) it can be seen that in all of the decomposition reactions NCs are formed. In agreement with the XRD analyses, the particle sizes were determined to be 5.2(1.2) nm and 2.6(0.5) nm for ThO_2 and PuO_2 respectively. In the case of UO_2, two different distributions could be found. One of them, the most prevalent, had an average particle size of 13.7(3.8) nm, and a second one, less numerous, but representing an important fraction of the sample, for which the average size was found to be 5.5(1.1) nm. From both XRD and TEM analyses it is obvious that the crystallinity of the samples is high, which is shown in the XRD by the diffraction peaks being visible up to high angle and in the high resolution TEM the planes in the crystallites are resolved (**Figs. 1** and **2**). The shape of the crystals, together with their increased reactivity, enables the consolidation of homogeneous nanostructured mixed oxides (MOX) as intermediates towards very dense nuclear fuels for GenIV reactors.

4 Conclusions and Perspectives

In conclusion, we present here for the first time the synthesis of highly crystalline, reactive nanograins of AnO_2 (*An*= Th, U, Pu) through the hydrothermal decomposition of the corresponding actinide(IV) oxalate hydrates. The particles produced in this method are significantly smaller than those produced by conventional thermal decomposition, where temperatures up to 600 °C are needed. Furthermore, the morphology differs as well. The process proved to be quantitative, facile, fast, and reproducible. It contains fewer procedural steps than typical oxalate precipitation/ decomposition processes [31], being suitable for production using a single vessel and under continuous flow. Ongoing experiments focus on the process optimisation, scale-up, and proving its flexibility in the production of MOX nanoparticles. As process temperatures below 250 °C are selective towards the actinide elements it could exhibit a certain application potential for the removal of uranium from contaminated wastewaters at the front-end of the nuclear fuel cycle but more attention has to be addressed to the kinetics and influences of other process parameters like pH or additional salt impurities in the system.

Acknowledgement: We are very grateful to Mr Daniel Bouëxière for the performance of XRD measurements on the PuO_2 NCs.

References

[1] Hodes G., When small Is different: Some recent advances in concepts and applications of nanoscale phenomena, Adv. Mater., 2007, 19, 639-655.
[2] de Mello Donegá C., Nanoparticles - Workhorses of nanoscience, Springer-Verlag Berlin Heidelberg, 2014.
[3] Sengupta A., Sarkar C.K., Introduction to nano, Springer-Verlag Berlin Heidelberg, 2015.
[4] Novikov A.P., Kalmykov S.N., Utsunomiya S., Ewing R.C., Horreard F., Merkulov A., et al., Colloid transport of plutonium in the far-field of the Mayak Production Association, Russia, Science, 2006, 314, 638-641.
[5] Kersting A.B., Efurd D.W., Finnegan D.L., Rokop D.J., Smith D.K., Thompson J.L., Migration of plutonium in groundwater at the Nevada Test Site, Nature, 1999, 397, 56 -59.
[6] Zänker H., Weiss S., Hennig C., Brendler V., Ikeda-Ohno A., Oxyhydroxy silicate colloids: A new type of waterborne actinide(IV) colloids, Chemistry Open, 2016, 5, 174-182.
[7] Zhang Z.T., Konduru M., Dai S., Overbury S.H., Uniform formation of uranium oxide nanocrystals inside ordered mesoporous hosts and their potential applications as oxidative catalysts, Chem. Commun., 2002, 2406-2407.
[8] Burns P.C., Kubatko K.A., Sigmon G., Fryer B.J., Gagnon J.E., Antonio M.R., et al., Actinyl peroxide nanospheres, Angew. Chem. Int. Ed., 2005, 44, 2135-2139.
[9] Wu H.M., Yang Y.G., Cao Y.C., Synthesis of colloidal uranium-dioxide nanocrystals, J. Am. Chem. Soc., 2006, 128, 16522-16523.
[10] Krivovichev S.V., Burns P.C., Tananaev I.G., Myasoedov B.F., Nanostructured actinide compounds, J. Alloys Compd., 2007, 444-445, 457-463.
[11] Soderholm L., Almond P.M., Skanthakumar S., Wilson R.E., Burns P.C., The structure of the plutonium oxide nanocluster $[Pu_{38}O_{56}Cl_{54}(H_2O)_8]^{14-}$, Angew. Chem. Int. Ed., 2008, 47, 298-302.
[12] Wang G.Q., Li G.D., Xu S., Li J.X., Chen J.S., Synthesis of uranium oxide nanoparticles and their catalytic performance for benzyl alcohol conversion to benzaldehyde, J. Mater. Chem., 2008, 18, 1146-1152.
[13] Rousseau G., Fattahi M., Grambow B., Desgranges L., Boucher F., Ouvrard G., et al., Synthesis and characterization of nanometric powders of UO_{2+x}, $(Th,U)O_{2+x}$ and $(La,U)O_{2+x}$, J. Solid State Chem., 2009, 182, 2591-2597.
[14] Ling J., Qiu J., Sigmon G.E., Ward M., Szymanowski J.E.S., Burns P.C., Uranium pyrophosphate/ methylenediphosphonate polyoxometalate cage clusters, J. Am. Chem. Soc., 2010, 132, 13395-13402.
[15] Biswas B., Mougel V., Pécaut J., Mazzanti M., Base-driven assembly of large uranium oxo/hydroxo clusters, Angew. Chem. Int. Ed., 2011, 50, 5745-5748.
[16] Wilson R.E., Skanthakumar S., Soderholm L., Separation of plutonium oxide nanoparticles and colloids, Angew. Chem. Int. Ed., 2011, 50, 11234-11237.
[17] Unruh D.K., Ling J., Qiu J., Pressprich L., Baranay M., Ward M., et al., Complex nanoscale cage clusters built from uranyl polyhedra and phosphate tetrahedral, Inorg. Chem., 2011, 50, 5509-5516.
[18] Wu H., Chen O., Zhuang J., Lynch J., LaMontagne D., Nagaoka Y., et al., Formation of heterodimer nanocrystals: UO_2/In_2O_3 and $FePt/In_2O_3$, J. Am. Chem. Soc., 2011, 133, 14327-14337.
[19] Nenoff T.M., Jacobs B.W., Robinson D.B., Provencio P.P., Huang J., Ferreira S., et al., Synthesis and low-temperature in situ sintering of uranium oxide nanoparticles, Chem. Mater., 2011, 23, 5185-5190.
[20] Hudry D., Apostolidis C., Walter O., Gouder T., Courtois E., Kübel C., et al., Non-aqueous synthesis of isotropic and anisotropic actinide oxide nanocrystals, Chem. Eur. J., 2012, 18, 8283-8287.
[21] Hudry D., Apostolidis C., Walter O., Gouder T., Janβen A., Courtois E., et al., Synthesis of transuranum-based nanocrystals via the thermal decomposition of actinyl nitrates, RSC Advances, 2013, 3, 18271-18274.
[22] Hudry D., Apostolidis C., Walter O., Gouder T., Courtois E., Kübel C., et al., Controlled synthesis of thorium and uranium oxide nanocrystals, Chem. Eur. J., 2013, 19, 5297-5305.
[23] Hudry D., Apostolidis C., Walter O., Janβen A., Manara D., Griveau J.C., et al., Ultra small plutonium oxide nanocrystals: An innovative material in plutonium science, Chem. Eur. J., 2014, 20, 10431-10438.
[24] Hudry D., Griveau J.C., Apostolidis C., Walter O., Colineau E., Rasmussen G., et al., Thorium/ uranium mixed oxide nanocrystals: Synthesis, structural characterisation and magnetic properties, Nano Research, 2014, 7, 119-131.

[25] Murray C.B., Norris D.J., Bawendi M.G., Synthesis and characterization of nearly monodisperse CdE (E= sulphur, selenium, tellurium) semiconductor nanocrystallites, J. Am. Chem. Soc., 1993, 115, 8706-8715.
[26] Murray C.B., Kagan C.R., Bawendi M.G., Synthesis and characterization of monodisperse nanocrystals and close-packed nanocrystal assemblies, Annu. Rev. Mater. Sci., 2000, 30, 545-610.
[27] Park J., Joo J., Kwon S.G., Jang Y., Hyeon T., Synthesis of monodisperse spherical nanocrystals, Angew. Chem. Int. Ed., 2007, 46, 4630-4660.
[28] Clavier N., Hingant N., Rivenet M., Obbade S., Dacheux N., Barré N., et al., X-ray diffraction and μ-Raman investigation on the monoclinic-orthorhombic phase transition in $Th_{1-x}U_x(C_2O_4)_2 \cdot 2H_2O$ solid solution, Inorg. Chem., 2010, 49, 1921-1931.
[29] Jovani Abril R., Eloirdi R., Bouëxière D., Malmbeck R., Spino J., In situ high temperature X-ray diffraction study on UO_2 nanoparticles, J. Mater. Sci., 2011, 46, 5-10.
[30] Jovani-Abril R., Gibilaro M., Janβen A., Eloirdi R., Somers J., Spino J., et al., Synthesis of nc-UO_2 by controlled precipitation in aqueous phase, J. Nucl. Mater., 2016, 477, 298-304.
[31] Tyrpekl V., Vigier J.F., Manara D., Wiss T., Dieste Blanco O., Somers J., Low-temperature decomposition of U(IV) and Th(IV) oxalates to nanograined oxide powders, J. Nucl. Mater., 2015, 460, 200-208.
[32] Adschiri T., Kanazawa K., Arai K., Rapid and continuous hydrothermal crystallization of metal oxide particles in supercritical water, J. Am. Ceram. Soc., 1992, 75, 1019–1022.
[33] Fang Z., Rapid production of micro- and nano-particles using supercritical water, Springer-Verlag Berlin Heidelberg, 2010.
[34] Türk M., Particle formation with supercritical fluids: Challenges and limitations, Elsevier London, 2014.
[35] Dunne P.W., Starkey C.L., Munna A.S., Tang S.V.Y., Luebben O., Shvets I., et al., Bench- and pilot-scale continuous-flow hydrothermal production of barium strontium titanate nanopowders, Chem. Eng. J., 2016, 289, 433-441.
[36] Makwana N.M., Tighe C.J., Gruar R.I., McMillan P.F., Darr J.A., Pilot plant scale continuous hydrothermal synthesis of nano-titania; effect of size on photocatalytic activity, Mat. Sci. Semicond. Processing, 2016, 42, 131-137.
[37] Jenkins I.L., Waterman M.J., The thermal decomposition of plutonium(IV) oxalate, J. Inorg. Nucl. Chem., 1964, 26, 131-137.